AMERICAN SOCIETY FOR MICROBIOLOGY | Journal of Virology®

VIRUS-CELL INTERACTIONS

Modulation of SOCS3 Levels via STAT3 and Estrogen-ERαp66 Signaling during Hepatitis E Virus Replication in Hepatocellular Carcinoma Cells

Harini Sooryanarain,[a,b] C. Lynn Heffron,[b] Hassan M. Mahsoub,[b] Anna M. Hassebroek,[b] Bo Wang,[b] Debin Tian,[b] S. Ansar Ahmed,[a,b] Xiang-Jin Meng[a,b]

[a]Center for Emerging, Zoonotic and Arthropod-borne Pathogens, Virginia-Maryland College of Veterinary Medicine, Virginia Polytechnic Institute and State University, Blacksburg, Virginia, USA

[b]Department of Biomedical Sciences and Pathobiology, Virginia-Maryland College of Veterinary Medicine, Virginia Polytechnic Institute and State University, Blacksburg, Virginia, USA

ABSTRACT Hepatitis E virus (HEV) infection usually results in a self-limiting acute disease; however, in infected pregnant women, it is associated with increased mortality and fulminant hepatic failure. Estrogen is known to be elevated during pregnancy, and estrogen signaling via classical estrogen receptor-ERα is known to regulate hepatocyte function and host innate immune response, including the STAT3 pathway. In this study, we investigated whether the estrogen classical signaling pathway via ERαp66 has any effect on STAT3 activation during HEV replication and HEV-induced IFN response. We first demonstrated that Huh7-S10-3 liver cells expressed the nonfunctional estrogen receptor ERαp36 isoform and lack the functional ERαp66 isoform. We further showed persistent phosphorylated-STAT3 levels in genotype 3 human HEV (Kernow P6 strain) RNA-transfected cells at later time points. In Huh7-S10-3 cells, estrogen at first-to-third trimester concentration (7.3 to 73 nM) did not significantly affect HEV replication; however, blocking of STAT3 activation led to a decrease in the HEV ORF2 protein level. Our mechanistic study revealed that STAT3 differentially regulates SOCS3 and type-III interferon (IFN) levels during HEV replication and the presence of estrogen-ERαp66 signaling stabilizes SOCS3 levels *in vitro*. We also demonstrate that HEV infection in pregnant and nonpregnant rabbits led to a significant increase in IFN response as measured by increased levels of IFN-stimulated-gene-15 (ISG15) mRNA levels irrespective of pregnancy status. Collectively, the results indicate that estrogen signaling and STAT3 regulate SOCS3 and IFN responses *in vitro* during HEV replication. The results have important implications for understanding HEV replication and HEV-induced innate immune response in pregnant women.

IMPORTANCE Hepatitis E is usually a self-resolving acute disease; however, in pregnant women, HEV infection is associated with high mortality and fulminant hepatic failure. During pregnancy, estrogen levels are elevated, and in the liver, the estrogen receptor ERα is predominant and estrogen signaling is known to regulate hepatocyte metabolism and leptin-induced STAT3 levels. Viruses can module host innate immune response via STAT3. Therefore, in this study, we investigated whether STAT3 and estrogen-classical signaling via the ERαp66 pathway modulate HEV replication and HEV-induced innate immune response. We demonstrated that estrogen signaling did not affect HEV replication in human liver cells, but blocking of STAT3 activation reduced HEV capsid protein levels in human liver cells. We also showed that inhibition of STAT3 activation reduced SOCS3 levels, while the presence of the estrogen-ERαp66 signaling pathway stabilized SOCS3 levels. The results from this study will aid our understanding of the mechanism of HEV pathogenesis and immune response during pregnancy.

Editor J.-H. James Ou, University of Southern California

Address correspondence to Xiang-Jin Meng, xjmeng@vt.edu.

The authors declare no conflict of interest.

Received 27 June 2022
Accepted 26 August 2022
Published 14 September 2022

KEYWORDS estrogen, STAT3, SOCS3, hepatitis E virus (HEV), replication, pregnancy, genotype 3 HEV

Hepatitis E virus (HEV) is a single-stranded, positive-sense, RNA virus, belonging to the family *Hepeviridae* (1). Extensive genetic divergence has been reported among known HEV strains (2), and at least 8 genotypes and 36 subtypes have been reported within the species *Orthohepevirus A* of the family (3), of which genotypes 1 to 4 are of importance to human health (4). HEV infection usually causes self-resolving acute hepatitis with <1% mortality (4, 5). However, during pregnancy, HEV infection can result in acute liver failure and higher mortality of up to 20 to 30% (6). Adverse pregnancy outcomes, including miscarriage and stillbirth, have been reported in genotype 1 HEV-infected women (7) and in genotypes 3 and 4 HEV-infected female rabbits (8, 9). It has been reported that HEV-infected pregnant women had higher levels of estradiol compared with uninfected women and estradiol treatment led to an increase in genotype 4 HEV replication *in vitro* (10). However, the underlying mechanism as to how estrogen affects HEV replication in hepatocytes remains unclear.

Estrogen imparts cell regulatory effects via classical and nonclassical pathways (11). Estrogen mediates the nonclassical signaling pathway by activating various host cellular kinases, including phosphatidylinositol 3-kinase-AKT (PI3K-AKT), extracellular signal-regulated kinase-mitogen-activated protein kinase (ERK-MAPK), p38-MAPK, and phospholipase C-protein kinase C (PLC-PKC), to exert a rapid effect on the cell. It was reported that HEV regulated estrogen signaling by inhibiting the PI3K and protein kinase A (PKA) pathways (12). In addition to the nonclassical pathway, estrogen also mediates the classical signaling pathway through the function the estrogen receptors ERα and ERβ (13). ERα receptor exists in three isoforms, ERαp66, ERαp46, and ERα36, of which the ERαp66 is the functional receptor involved in estrogen-mediated signaling (13). The ERβ receptor has five known isoforms, and the shorter isoforms of ERβ lack the C-terminal ligand-binding domain compared to the full-length ERβ isoform (11). ERα and ERβ differ in their distribution profile in various host tissues, and in the liver, ERα is predominant (14). Estrogen signaling via ERα has been shown to regulate hepatic function, including gluconeogenesis and lipid metabolism in mice (15). ERα signaling is also known to regulate leptin-induced STAT3 in HepG2 hepatocarcinoma cells (16).

STAT3 is a transcription factor that has multifaceted roles from cell cycle regulation to inflammatory response modulation (17). STAT3 can modulate virus-induced interferon (IFN) response and thus host innate antiviral response (18, 19). Additionally, overexpression of HEV ORF3 protein reportedly inhibited STAT3 translocation into the nucleus (20). However, the exact role of STAT3 in HEV replication and HEV-induced IFN response is unknown. Therefore, in this study, we investigated whether the estrogen classical signaling pathway via ERαp66 has any effect on STAT3 activation during HEV replication and HEV-induced IFN response. We demonstrated that STAT3 differentially regulates SOCS3 and type-III IFN levels during HEV replication and the presence of estrogen-ERαp66 signaling stabilizes SOCS3 levels.

RESULTS

Huh7-S10-3 hepatocellular carcinoma cells lack functional isoform of estrogen receptor ERαp66. We showed that Huh7-S10-3 cells, which support productive HEV replication, are devoid of the functional isoform of the estrogen receptor ERαp66 but strongly express ERαp36, a nonfunctional isoform of ERα (Fig. 1A and B). Therefore, in this study, we decided to use the ERαp66 overexpression model to study the role of the estrogen-ERαp66 signaling pathway during HEV replication. To standardize the ERαp66 overexpression, we first determined the stability of ERαp66 protein, as high levels of ERαp36 have been reported to reduce ERαp66 protein levels (11). We used green fluorescent protein (GFP) as our control and monitored ERαp66 and GFP protein expressions in the presence or absence of a 7.3-nM concentration of estrogen, at 1 to 10 days posttransfection (dpt). Our results showed that the stability of ERαp66 was reduced at later time points and estrogen treatment also further reduced the ERαp66

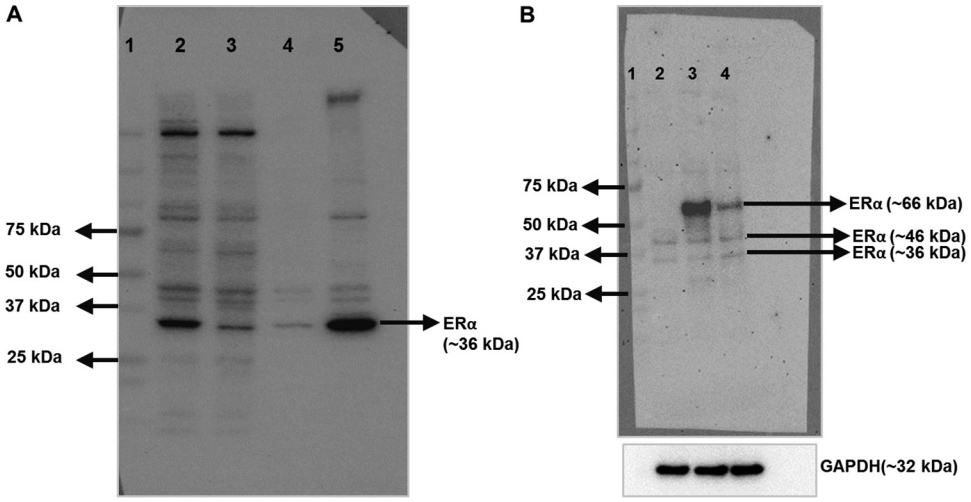

FIG 1 Huh7-S10-3 hepatocellular carcinoma cells lack functional isoform of estrogen receptor ERαp66. (A) Western blot analyses of classical estrogen receptor ERα in Huh7-S10-3 cells (lane 2), HepG2-C3A cells (lane 3), JEG3 cells (lane 4; a known ERα-negative cell line), and IPECJ2 cells (lane 5). (B) Huh7-S10-3 cells (lane 2), Huh7-S10-3 cells transfected with pCMV-ERαp66 at 24 h posttransfection (lane 3), and 48 h posttransfection (lane 4). For panels A and B, lane 1 is the marker (All-blue marker; Bio-Rad; cat. no. 1610373).

expression (Fig. 2), while GFP protein remained unaffected in all the tested conditions. Due to the ERαp66 stability concern, we were unable to establish a stable cell line overexpressing ERαp66; hence, in this study, we decided to use the thetransient-transfection approach to study ERαp66-mediated estrogen signaling during HEV replication. We measured phosphorylation of ERK using Western blot and estrogen-response-element (ERE)-firefly luciferase reporter assay to determine the estrogen-mediated nonclassical pathway and classical pathway, respectively, in Huh7-S10-3 cells (Fig. S1). Our results showed that estrogen induced the nonclassical pathway in Huh7-S10-3 cells and ERαp66 overexpression led to enhanced ERE-luciferase activity during estrogen treatment, while ERE-luciferase activity remained undetected in GFP-overexpressing cells even in the presence of estrogen. This shows that estrogen induced the classical pathway only under ERαp66 overexpression and that ERαp66 is functional.

STAT3 phosphorylation increases as HEV replication progresses independent of estrogen receptor ERαp66. We determined STAT3 activation levels at various time points, from 30 min to 7 days post-HEV RNA transfection (dpt) in Huh7-S10-3 liver cells,

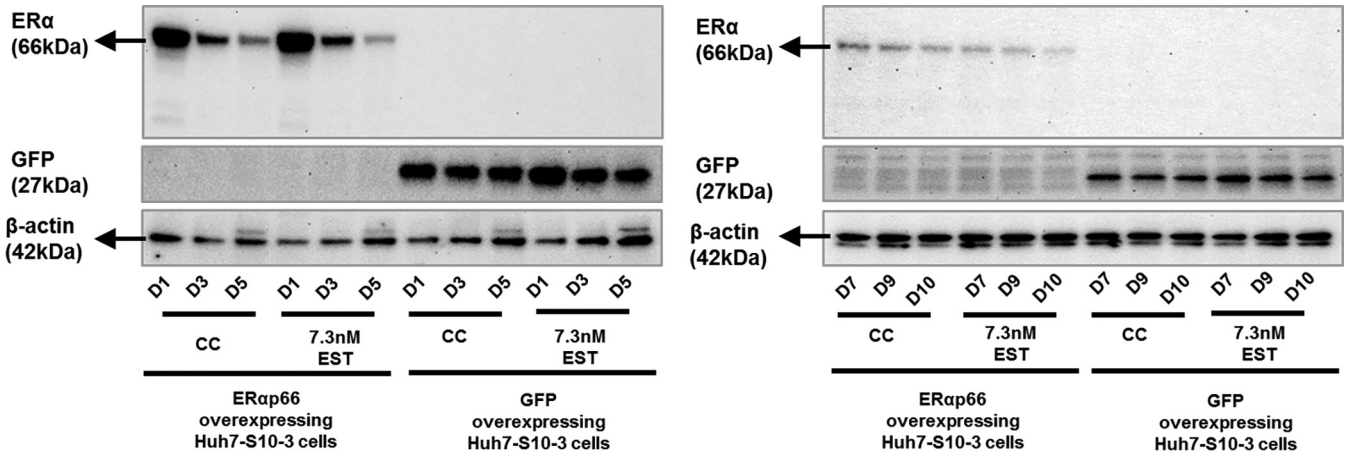

FIG 2 Overexpression of ERαp66 in the presence or absence of first-trimester concentration of estrogen (7.3 nM estrogen). A representative Western blot for ERαp66, GFP, and β-actin protein levels in cells transfected with pCMV-ERαp66 plasmid or with pcDNA-EGFP (vector control) in the presence or absence of 7.3 nM estrogen at various time points (D1 to D10, i.e., 1 to 10 days posttransfection). Lanes containing samples obtained from cell control without estrogen treatment are labeled as CC; lanes containing samples obtained from cells treated with 7.3 nM estrogen are labeled as 7.3 nM EST.

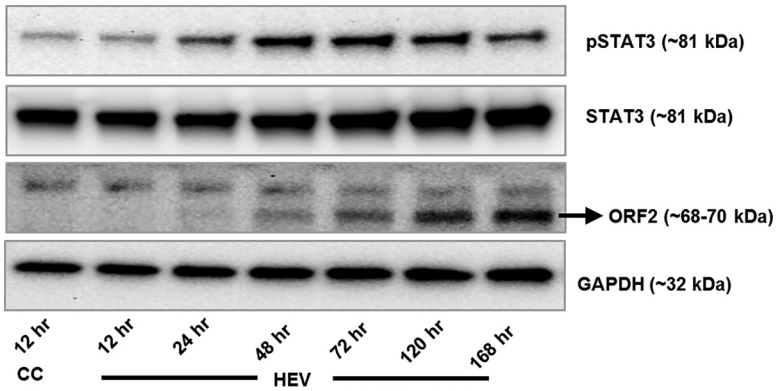

FIG 3 Time kinetics of increased STAT3 phosphorylation during HEV replication in HEV P6 RNA-transfected Huh7-S10-3 liver cells. A representative Western blot of pSTAT3, STAT3, HEV ORF2, and GAPDH protein levels in HEV P6 RNA-transfected Huh7-S10-3 cells at various time points. The sample obtained from cell control without HEV P6 transfection is labeled as CC; samples obtained from HEV P6 RNA-transfected cells are labeled as HEV.

by measuring phosphorylated-STAT3 (pSTAT3) using Western blot analysis. We did not observe any pSTAT3 at early time points between 30 min and 12 h (Fig. S2). We began to observe detectable levels of pSTAT3 from 3 dpt with HEV RNA, and these persisted until 7 dpt. We also found that the pSTAT3 levels correlated with an increased accumulation of HEV ORF2 capsid protein levels (Fig. 3).

We subsequently determined the levels of pSTAT3 expression in HEV RNA-transfected Huh7-S10-3 cells overexpressing functional estrogen receptor ERαp66 or GFP-overexpressing cells at various time points from 12 h to 7 dpt (i.e., 168 h). We found that overexpression of ERαp66 did not alter the pSTAT3 levels during HEV replication (Fig. 4). As expected, ERαp66 levels decreased at later time points. This result suggested that ERαp66 overexpression by itself did not have a significant effect on STAT3 activation during HEV replication. Thus, we proceeded to determine the potential effect of the estrogen nonclassical and classical signaling pathways in STAT3 activation and HEV replication.

The pSTAT3 and HEV ORF2 expression levels are not affected by first-trimester concentration of estrogen-mediated classical and nonclassical signaling pathways. To determine whether the estrogen nonclassical and classical signaling pathways have

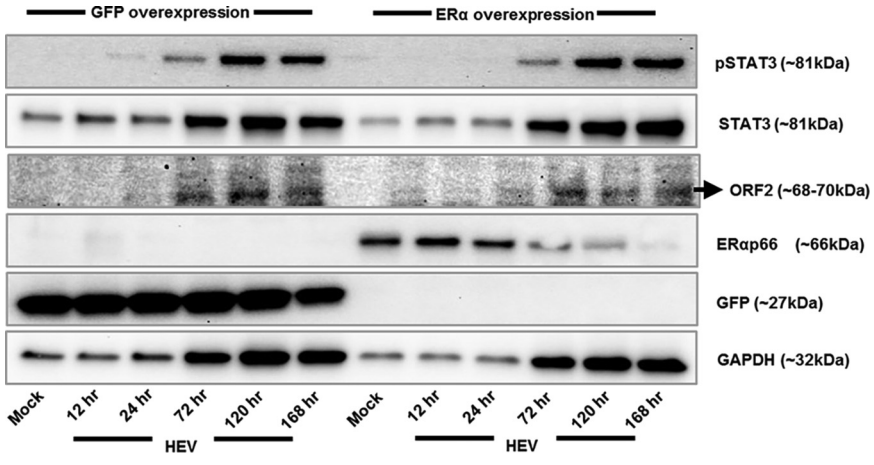

FIG 4 STAT3 phosphorylation increases as HEV replication progresses independent of estrogen receptor ERαp66. A representative Western blot of pSTAT3, STAT3, ERαp66, GFP, HEV ORF2, and GAPDH protein levels at various time points; $n = 2$ independent experiments. The sample obtained from mock control, i.e., cells without HEV P6 RNA transfection, is labeled as Mock; samples obtained from HEV P6 RNA-transfected cells are labeled as HEV. Time point is represented in hour (hr) post-HEV RNA transfection; 24 to 168 h is 1 to 7 days post-HEV RNA transfection. GFP overexpression, cells overexpressing GFP; ERα overexpression, cells overexpressing ERαp66.

TABLE 1 Physiological levels of estrogen (17β-estradiol) in serum during uncomplicated human pregnancy

Stage	Range (ng/ml[a])	Concn used in this study
First trimester	1.16–3.59 ng/ml	2 ng/ml (7.3 nM estrogen [EST])
Second trimester	5.33–15.1 ng/ml	10 ng/ml (37 nM EST)
Third trimester	12.8–32.9 ng/ml	20 ng/ml (73 nM EST)

[a]From Schock et al. (26).

any effect on pSTAT3 and HEV ORF2 expression levels, the Huh7-S10-3 human liver cells overexpressing GFP (vector control) or ERαp66 (functional estrogen receptor) were transfected with full-length HEV genomic RNAs transcribed from the genotype 3 (Gt3) HEV P6 infectious clone in the presence or absence of 7.3 nM estrogen. We chose to use a 7.3-nM concentration of estrogen because it is the average level of estrogen present during the first trimester of pregnancy (Table 1). The pSTAT3 and HEV ORF2 levels were determined using Western blot analyses at various time points from 1 to 7 dpt with HEV RNA.

Our results showed persistent levels of pSTAT3 expression in tested conditions. HEV ORF2 protein levels remained similar between all the test conditions irrespective of estrogen treatment (Fig. 5A). To further confirm our results of HEV ORF2 protein expression levels, we used HEV-specific reverse transcription-quantitative PCR (RT-qPCR) to determine HEV RNA levels at 5 dpt. In concordance with Western blot analyses, HEV RNA levels were also similar between all the conditions tested irrespective of estrogen treatment (Fig. 5B).

Since our experimental model in the study is HEV RNA transfection, we then further tested if the HEV RNA pathogen-associated molecular pattern has any effect on STAT3 signaling rather than HEV replication using HEV-P6 infectious virus infection and HEV-P6 GAD RNA (a replication-deficient HEV-P6 clone) along with HEV-P6 RNA transfection. Our results showed a higher pSTAT3 level at D5 postinfection or post-HEV RNA-transfection compared to D1 (Fig. S3). In concordance with our previous experiment (Fig. 5A), we observed a persistent pSTAT3 expression in all the conditions tested irrespective of HEV replication and estrogen signaling (Fig. 5C). Therefore, this result shows that estrogen at the first-trimester concentration did not affect HEV ORF2 protein levels and that there is a persistent pSTAT3 expression irrespective of HEV replication.

Inhibition of STAT3 activation decreases HEV ORF2 protein expression levels and stabilized ERαp66 levels during the estrogen signaling pathway. Since we consistently observed a persistent activation of STAT3 irrespective of HEV replication in our experiments, and we had a detectable level of HEV ORF2 protein expression in the HEV RNA transfection model, we then sought to determine the role of STAT3 activation in HEV ORF2 expression levels during the estrogen nonclassical and classical signaling pathway. We determined the HEV ORF2 expression levels in 7.3 nM estrogen-treated Huh7-S10-3 cells overexpressing GFP or ERαp66 in the presence or absence of a STAT3 activation inhibitor (S3I-201).

First, we tested various concentrations of STAT3 activation inhibitor (17.5 μM, 35 μM, and 70 μM) to determine (i) cell viability at 48 h treatment using a WST assay (Fig. S4A) and (ii) the optimal concentration to inhibit STAT3 activation during HEV RNA transfection (Fig. S4B) in both GFP- and ERαp66-overexpressing cells without estrogen treatment. Our results showed that treatment with STAT3 activation inhibitor at various concentrations by itself did not induce loss of cell viability at 48 h (Fig. S4A) and at a 70-μM concentration resulted in a consistent inhibition of pSTAT3 levels in all the conditions tested during HEV RNA transfection (Fig. S4B). Hence, all further experiments were done by using a 70-μM STAT3 inhibitor concentration.

We demonstrated that blocking of STAT3 activation resulted in decreased HEV ORF2 protein levels and an increase in ERαp66 protein levels at 5 dpt with HEV RNA (Fig. 6A). Additionally, we also tested SOCS3 and cyclin-D1 protein expression levels under these conditions, as both STAT3 signaling (21) and ERα signaling (22) are known to affect SOCS3 protein expression to regulate immunomodulation; both the STAT3 pathway (23)

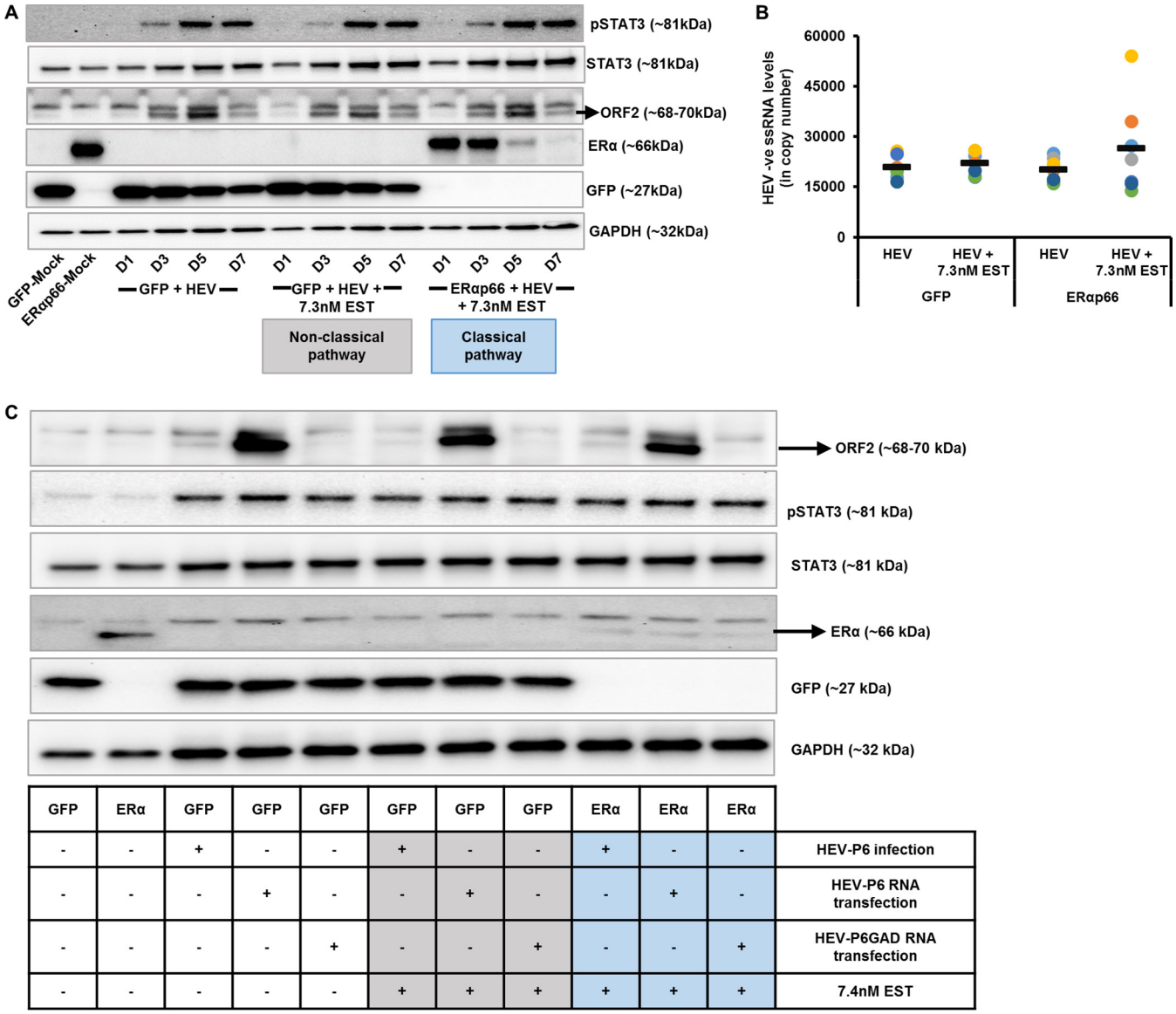

GFP	ERα	GFP	GFP	GFP	GFP	GFP	GFP	ERα	ERα	ERα	
-	-	+	-	-	+	-	-	+	-	-	HEV-P6 infection
-	-	-	+	-	-	+	-	-	+	-	HEV-P6 RNA transfection
-	-	-	-	+	-	-	+	-	-	+	HEV-P6GAD RNA transfection
-	-	-	-	-	+	+	+	+	+	+	7.4nM EST

FIG 5 pSTAT3 levels and HEV ORF2 levels remained unaffected by first-trimester concentration of the estrogen-mediated classical and nonclassical signaling pathways. (A) A representative Western blot of pSTAT3, STAT3, ERαp66, GFP, HEV ORF2, and GAPDH protein levels at various indicated time points. D1 to D7 is 1 to 7 days post-HEV RNA transfection; 7.3 nM EST is 7.3 nM estrogen treatment; $n = 2$ independent experiments. Mock, control cells without any treatment; GFP-Mock, mock control of GFP-overexpressing cells; ERαp66-Mock, mock control of ERαp66-overexpressing cells at D1; GFP + HEV, GFP-overexpressing cells transfected with HEV P6 RNA; ERαp66 + HEV, ERαp66-overexpressing cells transfected with HEV P6 RNA; Nonclassical pathway, estrogen treatment under GFP overexpression is considered to represent estrogen nonclassical pathway signaling; Classical pathway, estrogen treatment under ERαp66-overexpressing cells is considered to represent estrogen classical signaling pathway. (B) HEV RNA levels at day 5 post-HEV RNA transfection as determined by negative-strand HEV RNA RT-qPCR. Each dot represents one independent experiment, and mean is represented as thick black line; $n = 7$ independent experiments. (C) Representative Western blot of pSTAT3, STAT3, ERαp66, GFP, HEV ORF2, and GAPDH protein levels at 5 days post-HEV-P6 infectious virus infection, HEV-P6 RNA transfection, or HEV-P6-GAD (replication deficient) RNA transfection under various test conditions. GFP, GFP-overexpressing cells; ERαp66, ERαp66-overexpressing cells; HEV, HEV-P6 RNA-transfected cells; HEV + 7.3 nM EST, 7.3 nM estrogen-treated HEV-P6 RNA-transfected cells.

and estrogen (24) are also known to regulate cell cycle through cyclin-D1 levels. At 5 dpt with HEV RNA, we found that the presence of 70 μM STAT3 inhibitor resulted in decreased SOCS3 and cyclin-D1 protein levels during HEV replication (Fig. 6A). We also measured the HEV RNA levels using RT-qPCR and showed that STAT3 inhibitor treatment decreased HEV RNA levels in 7.3 nM estrogen-treated conditions (Fig. 6B).

Both estrogen-mediated ERαp66 signaling and STAT3 regulate SOCS3 expression levels during HEV replication *in vitro*. To understand how various levels of estrogen affect HEV replication and HEV-induced IFN response, we determined the effect of

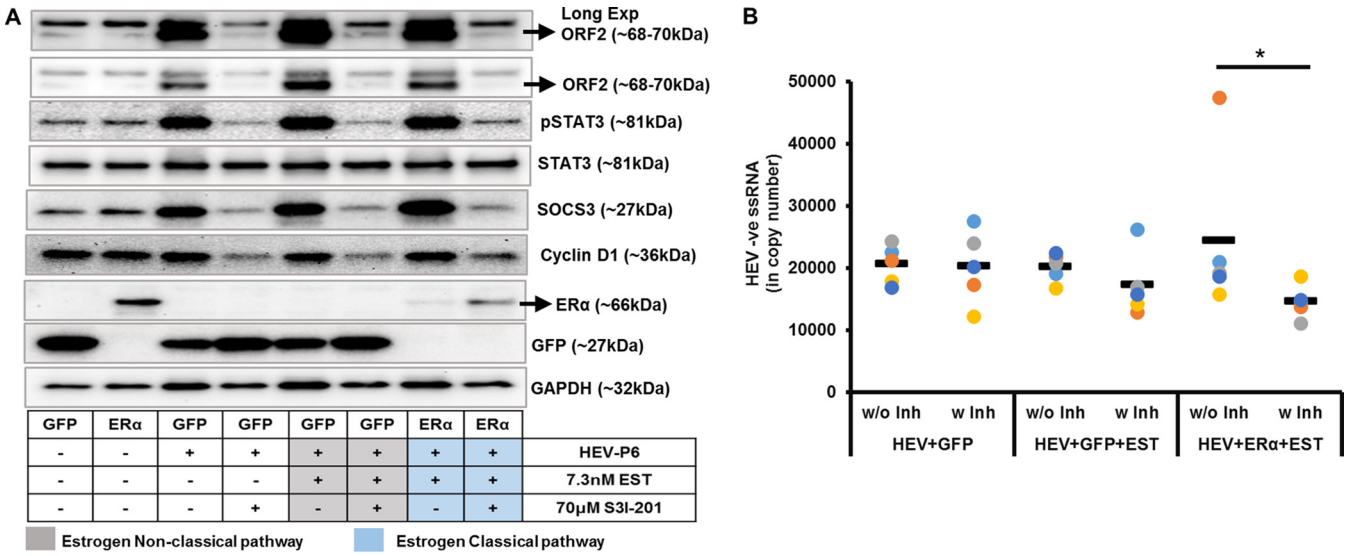

FIG 6 Inhibition of STAT3 activation reduces HEV ORF2 protein levels and stabilizes ERαp66 levels during the estrogen signaling pathway. (A) A representative Western blot of pSTAT3, STAT3, SOCS3, cyclin-D1, ERαp66, GFP, HEV ORF2, and GAPDH protein levels at day 5 post-HEV RNA transfection under various conditions tested in the presence or absence of 70 μM STAT3 inhibitor (S3I-201); n = 2 to 3 independent experiments. Estrogen Nonclassical pathway, estrogen treatment under GFP overexpression is considered to represent estrogen nonclassical pathway signaling; Estrogen Classical pathway, estrogen treatment under ERαp66-overexpressing cells is considered to represent estrogen classical signaling pathway. (B) HEV RNA levels at day 5 post-HEV P6 RNA transfection as determined by negative-strand HEV RNA RT-qPCR under various conditions tested with 70 μM STAT3-inhibitor (w Inh) or without 70 μM STAT3-inhibitor (w/o Inh) treatment, EST (7.3 nM estrogen) treatment; HEV + GFP, GFP-overexpressing cells transfected with HEV P6 RNA; HEV + ERα, ERαp66-overexpressing cells transfected with HEV P6 RNA. Each dot represents one independent experiment, and mean is represented as a thick black line; n = 5 independent experiments, *, $P \leq 0.05$, ANOVA with *post hoc* Student's t test.

different concentrations of estrogen that are typically seen during the first (7.3 nM), second (37 nM), and third (73 nM) trimester of pregnancy, respectively, on HEV replication and IFN responses in the presence or absence of 70 μM STAT3 inhibitor. We measured the HEV RNA, IFN-λ1, ISG15, SOCS3, and IL-6 mRNA levels using RT-qPCR to determine the effect of the estrogen-mediated ERα signaling-STAT3-SOCS3 axis on HEV replication and HEV-induced IFN response. RPS18 was used as a housekeeping gene.

Our results showed that HEV RNA levels (Fig. 7A) decreased during the presence of STAT3 inhibitor at first- and second-trimester concentration of estrogen-treated GFP-overexpressing cells. However, we observed a decrease in HEV RNA levels in first-trimester concentration of estrogen-treated ERαp66-overexpressing cells. Treatment with the third-trimester concentration of estrogen modulated the ability of the STAT3 inhibitor to decrease HEV RNA levels. In GFP-overexpressing cells, the third-trimester concentration of estrogen treatment led to a complete loss of STAT3 inhibitor-mediated decrease in HEV RNA levels, while in ERαp66-overexpressing cells the STAT3 inhibitor led to an increase in HEV RNA levels.

Consistent with our Western blot data, SOCS3 mRNA levels decreased in the presence of the STAT3 inhibitor under the condition tested during HEV replication (Fig. 7B). Interestingly, upon the STAT3 inhibitor treatment, the SOCS3 mRNA levels in ERαp66-overexpressing cells were significantly higher than that in GFP-overexpressing cells during HEV replication (Fig. 7B, inset). To further confirm the observation that estrogen-ERαp66 signaling mediates regulation of SOCS3 during HEV replication, we determined SOCS3 and cyclin-D1 protein expression levels in ERαp66- or GFP-overexpressing cells in the presence of estrogen and with various concentration of STAT3 inhibitor at 5 dpt of HEV RNA. Our results showed that a lower concentration of STAT3 inhibitor (35 μM) decreased SOCS3 protein levels during HEV replication under the estrogen-GFP condition, while SOCS3 levels remained high when estrogen-ERαp66 signaling was present (Fig. 7C). A lower concentration of the STAT3 inhibitor did not reduce cyclin-D1 levels; cyclin-D1 reduction was only seen during the 70-μM STAT3 inhibitor treatment. Interestingly, even a lower concentration of the STAT3 inhibitor decreased HEV ORF2

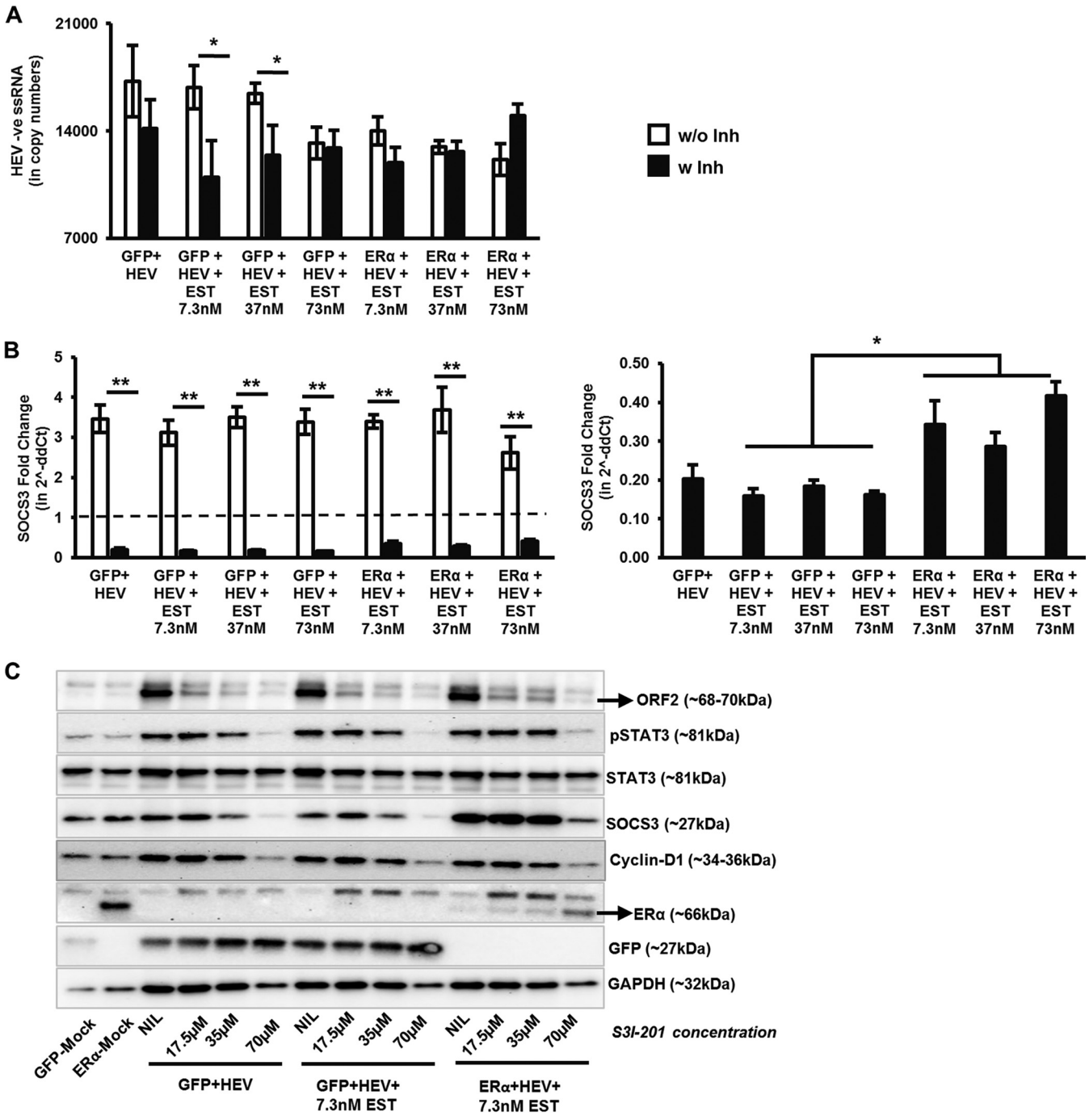

FIG 7 Both estrogen-mediated ERα signaling and STAT3 regulate SOCS3 mRNA levels during HEV replication *in vitro*. (A and B) Negative-strand HEV RNA (HEV-ve ssRNA) (A) and SOCS3 mRNA (B) levels as determined by gene-specific RT-qPCR. Open bars represent samples obtained from without 70 μM STAT3-inhibitor treatment (w/o Inh), and filled bars represent samples obtained from with 70 μM STAT3-inhibitor (w Inh) treatment. EST (estrogen) treatment concentration as indicated in the figure. GFP + HEV, GFP-overexpressing cells transfected with HEV P6 RNA; ERα + HEV, ERαp66-overexpressing cells transfected with HEV P6 RNA; n = 3 independent biological replicates tested twice. *, $P \leq 0.05$; **, $P \leq 0.01$ ANOVA with *post hoc* Student's t test (to compare STAT3 inhibitor treatment within a group) or Tukey test (to compare multiple groups among the STAT3 inhibitor-treated samples). Fold change was calculated using 2^-ddCT method as follows: RPS18 was used as housekeeping gene, for GFP set 2^-[(dCt GFP + HEV) − (dCt GFP − Mock)], for ERαp66 set 2^-[(dCt ERαp66 + HEV) − (dCt ERαp66 − Mock)]. Dashed line represents baseline gene expression in mock controls. (C) Representative Western blot of pSTAT3, STAT3, SOCS3, cyclin-D1, ERαp66, GFP, HEV ORF2, and GAPDH protein levels at day 5 post-HEV RNA transfection under various STAT3-inhibitor (S3I-201) concentrations tested as indicated; n = 2 independent experiments. Mock, control cells without any treatment; GFP-Mock, mock control of GFP-overexpressing cells; ERαp66-Mock, mock control of ERαp66-overexpressing cells at D1; GFP + HEV, GFP-overexpressing cells transfected with HEV P6 RNA; GFP + HEV + 7.3 nM EST, GFP-overexpressing cells transfected with HEV P6 RNA plus 7.3 nM estrogen treatment; ERαp66 + HEV + 7.3 nM EST, ERαp66-overexpressing cells transfected with HEV P6 RNA plus 7.3 nM estrogen treatment.

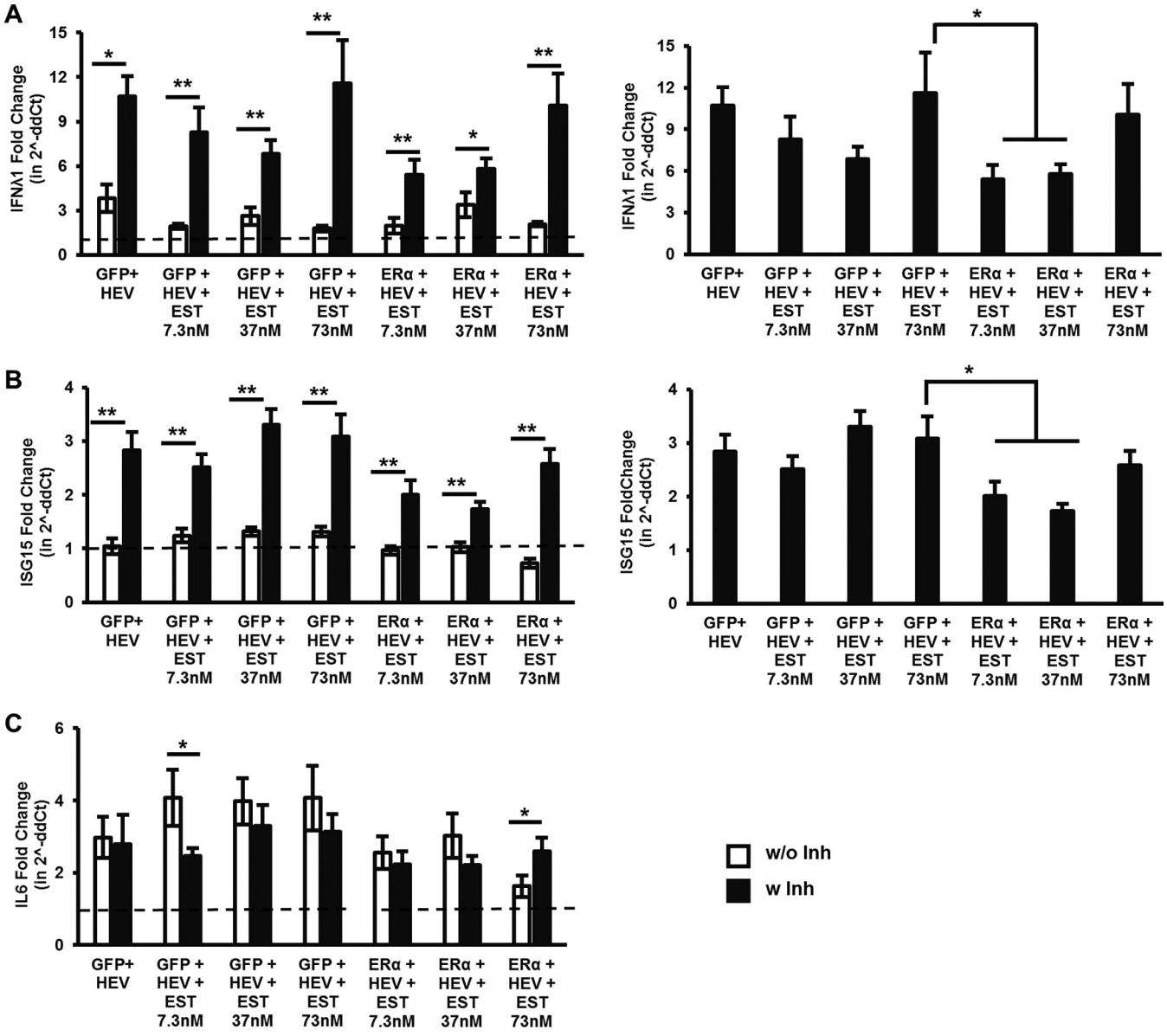

FIG 8 STAT3 inhibition enhances interferon response during HEV replication. (A to C) IFN-λ1 (A), ISG15 (B), and IL-6 mRNA (C) levels at day 5 post-HEV P6 RNA-transfected cells under various test conditions as determined by gene-specific RT-qPCR. Open bars represent samples obtained from without 70 μM STAT3-inhibitor treatment (w/o Inh), and filled bars represent samples obtained from with 70 μM STAT3-inhibitor (w Inh) treatment. EST (estrogen) treatment concentration as shown. GFP + HEV, GFP-overexpressing cells transfected with HEV P6 RNA; ERα + HEV, ERαp66-overexpressing cells transfected with HEV P6 RNA. Fold change was calculated using 2^-ddCT method as follows: RPS18 was used as housekeeping gene, for GFP set 2^-[(dCt GFP + HEV) − (dCt GFP − Mock)] and for ERαp66 set 2^-[(dCt ERαp66 + HEV) − (dCt ERαp66 − Mock)]. Dashed line represents baseline gene expression in mock controls; n = 3 independent biological replicates tested twice. *, $P \leq 0.05$; **, $P \leq 0.01$ ANOVA with *post hoc* Student's t test (to compare STAT3 inhibitor treatment within a group) or Tukey test (to compare multiple groups among the STAT3 inhibitor-treated samples).

protein levels. The result suggested that estrogen-ERαp66 signaling regulates SOCS3 levels during HEV replication, in addition to the STAT3 pathway.

We also found that STAT3 inhibition had an inverse effect between IFN-λ1 (Fig. 8A) and SOCS3 (Fig. 7B) levels. Inhibition of STAT3 activation resulted in increased IFN-λ1 (Fig. 8A) and a subsequent increased IFN-stimulated gene-15 (ISG15; Fig. 8B) mRNA levels, while SOCS3 (Fig. 7B) mRNA levels decreased under the tested conditions. We also measured IL-6 mRNA levels (Fig. 8C), as STAT3 can also be activated via IL-6 and SOCS3 is known to block IL-6-mediated STAT3 activation. However, we did not find any inverse effect between SOCS3 mRNA levels and IL-6 mRNA levels upon STAT3 inhibition during HEV replication. Taken together, these results suggest that both STAT3 and

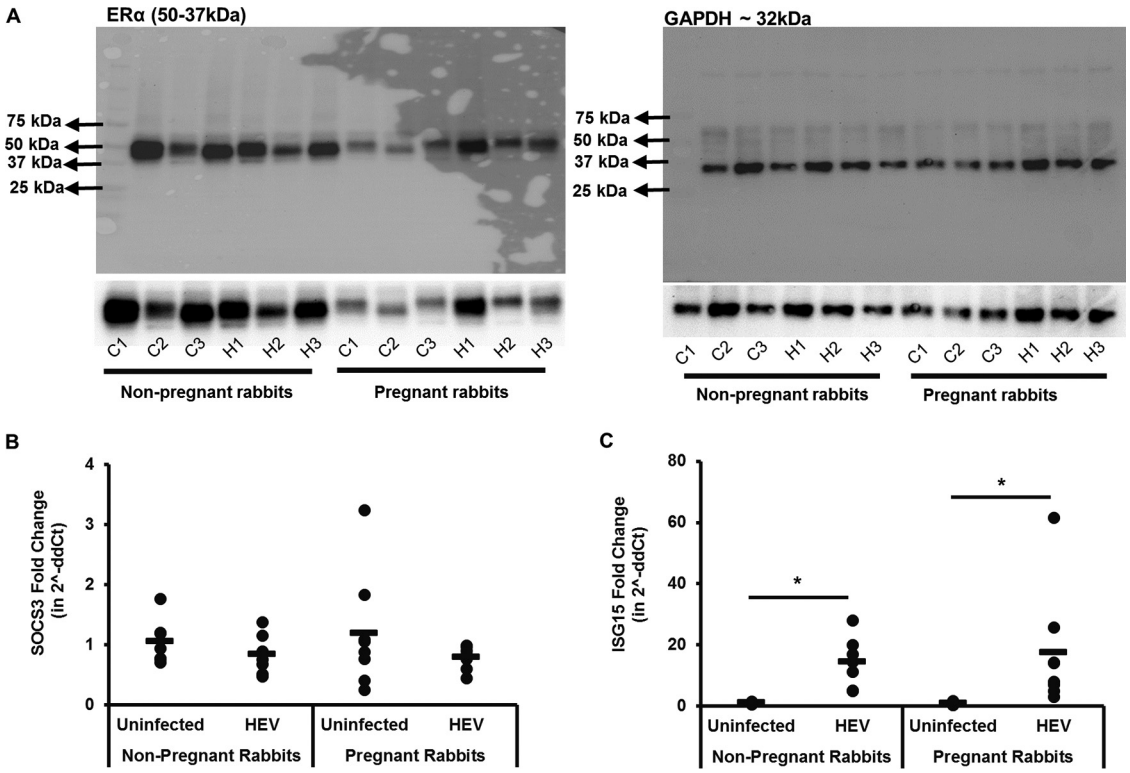

FIG 9 Increased ISG15 mRNA levels in the convenient liver tissues of HEV-infected rabbits irrespective of pregnancy status. (A) Representative western blot of ERαp66 and GAPDH in control and HEV-infected non-pregnant and pregnant rabbits (N = 3 from each group). (B) SOCS3, and (C) ISG15 mRNA levels as determined by gene-specific RT-qPCR in control and HEV-infected nonpregnant and pregnant rabbits at 4 weeks postinfection; n = 7 control nonpregnant rabbits, 7 HEV-infected nonpregnant rabbits, 8 control pregnant rabbits, and 8 HEV-infected pregnant rabbits. Each dot represents one individual animal, and thick black line represents mean. *, $P \leq 0.05$ as determined by F test.

estrogen-ERαp66 signaling regulate SOCS3 levels and thus plausibly modulate HEV-induced interferon response during pregnancy.

Increased levels of ISG15 in liver tissues of HEV-infected rabbits irrespective of pregnancy status. To test if our *in vitro* observation happens *in vivo*, we compared SOCS3 and IFN levels in convenient liver tissue samples from uninfected control and HEV-infected pregnant and nonpregnant rabbits (25) to determine if pregnancy modulates SOCS3 and interferon response levels during HEV infection. First, we determined ERα expression levels in uninfected and HEV-infected pregnant and nonpregnant rabbit liver samples (n = 3 from each set) using Western blot to determine the ERα isoform profile in female rabbit liver tissue. We did not observe the ERαp66 isoform; however, we detected ERα protein bands between 50 and 37 kDa (Fig. 9A), and the size of the ERα isoform slightly varied among donors.

We then quantified the SOCS3 and ISG15 mRNA levels in liver samples obtained from uninfected and HEV-infected nonpregnant rabbits and pregnant rabbits (n = 7 to 8 in each set), respectively. Unfortunately, we could not determine the IFN-λ mRNA levels in these samples as the rabbit IFN-λ gene is not annotated. IFN-β mRNA levels remained at undetectable levels; hence, we used ISG15 as a marker to measure IFN response in these liver tissue samples. Our results showed that SOCS3 (Fig. 9B) mRNA levels remained similar in uninfected and HEV-infected groups. However, we showed that HEV infection led to a significant increase in ISG15 (Fig. 9C) mRNA levels in liver tissues, irrespective of the pregnancy status of the rabbits.

DISCUSSION

HEV infection in pregnant women is associated with higher mortality and fulminant hepatic failure. Estrogen levels are elevated during pregnancy, and the estrogen receptor

ERα is predominant in liver, and estrogen signaling can regulate hepatocyte metabolism and leptin-induced STAT3 levels. In this study, we investigated whether the estrogen-ERαp66 signaling pathway and STAT3 modulate HEV replication by influencing HEV-induced innate immune response in Huh7-S10-3 hepatocellular carcinoma cells. We demonstrated that Huh7-S10-3 cells expressed a nonfunctional isoform of the classical estrogen receptor ERα (i.e., ERαp36) and lack the functional isoform of the classical estrogen receptor ERαp66. In Huh7-S10-3 cells, increased STAT3 activation levels were observed as HEV replication progressed. Pretreatment with estrogen (17β-estradiol) at the physiological concentration (2 to 20 ng/ml) typically seen during the first to third trimester of pregnancy did not affect HEV replication, while inhibition of STAT3 activation led to decreased HEV ORF2 protein levels. We also show that both STAT3 activation and overexpression of the estrogen-ERαp66 signaling pathway differentially modulate SOCS3, IFN-λ1, and ISG15 mRNA levels during HEV replication in Huh7-S10-3 cells.

17β-estradiol is the major estrogen in females. During uncomplicated pregnancy, serum 17β-estradiol levels vary from 2 to 31 ng/ml (26). Studies have shown increased levels of HEV RNA and seropositivity in pregnant women with fulminant hepatic failure compared to nonpregnant women with fulminant hepatic failure (27). It has also been reported that HEV regulates the estrogen-signaling pathway *in vitro* (12) and increased estrogen treatment enhanced HEV replication (10). In this present study, however, we showed that neither the presence of the estrogen nonclassical signaling pathway nor the presence of the estrogen classical signaling pathway had any significant effect on HEV replication levels. The difference between our present study and the previous *in vitro* study is that the previous study used the A549 human lung epithelial cell line and Gt-4 HEV strain, while in our present study we used the Huh7-S10-3 human liver cell line and Gt-3 HEV (P6 strain). Huh7-S10-3 cells are hepatocarcinoma cells and support productive HEV P6 replication (28). In hepatocarcinoma cells, it is known that ERαp36, the nonfunctional form of ERα, is expressed at higher levels (29, 30). Mechanistic studies have shown that ERαp36 can affect the stability of other functional estrogen receptors, including ERαp66 and ERβ (11, 31). Concurrently, in our present study, we demonstrated that overexpression of ERαp66 in Huh7-S10-3 cells did not result in a consistent stable expression of the full-length protein; instead, the ERαp66 protein expression level decreased over time. In cancer cells, ERα and ERβ levels have differential regulation of the cell cycle, and the ERα pathway is associated with cell proliferation, while ERβ pathway is associated with antiproliferation (32). Additionally, the *ex vivo* model has shown that the pathogenicity of HEV is genotype specific and that Gt-1 HEV induced severe tissue alterations and dysregulation of host soluble factors more efficiently compared to the less-pathogenic Gt-3 HEV (33). Therefore, the observed difference between our present study and the previous *in vitro* study could be due to a variation in the estrogen receptor profile in the cell line used and could also be possibly due to the different viral strain used.

It has been reported that HEV blocked the STAT3 pathway, as overexpression of HEV ORF3 is shown to block epidermal growth factor (EGF)-induced STAT3 translocation into the nucleus (20). However, in our present study, we observed increased levels of STAT3-phosphorylation during the late time points of HEV replication. We also observed that blocking of STAT3 activation by the S3I-201 inhibitor led to a decrease in HEV ORF2 protein levels. Viruses are known to use the STAT3 pathway to modulate innate immune response and host cell cycle (34). Studies have shown that STAT3 regulates both DNA and RNA viral replications. Hepatitis B virus activates STAT3 signaling to support viral replication and prevents infected cell apoptosis (35). Similarly, the varicella-zoster virus induced STAT3 phosphorylation, and treatment with S3I-201 impaired viral replication (36). In the present study, we showed that inhibition of STAT3 activation led to a decrease in HEV ORF2 protein. STAT3 and estrogen are known to impart immunosuppression via activating SOCS3 protein (37). It has been reported that enterovirus induces STAT3 activation to regulate type-I IFN-mediated antiviral response (38). HEV is known to induce a robust type-III IFN response both *in vitro* (39–41) and *in vivo*

(42). In this study, we demonstrated that inhibition of STAT3 activation led to decreased SOCS3 and increased HEV-induced IFN-λ1 and ISG15 mRNA levels. We also observed that the presence of estrogen-ERαp66 signaling enhanced SOCS3 expression levels. Therefore, taken together, we can possibly conclude that both STAT3 and estrogen-ERαp66 signaling pathways differentially influence HEV-induced innate immune response *in vitro*.

Impairment of TLR-mediated innate immune response has been reported in HEV-infected pregnant women (43) and in HEV-infected pregnant women with acute liver failure (44) compared to HEV-infected nonpregnant women. Moreover, it was reported that HEV has a genotype-specific sensitivity to IFN-mediated antiviral response in human placental cells (45). Therefore, in this study, we tested convenient liver tissues of HEV-infected pregnant and nonpregnant rabbits to determine if pregnancy influences HEV-induced IFN response and also to further validate our *in vitro* observations. Interestingly, our results showed that HEV induced higher levels of IFN response, as determined by ISG15 levels, irrespective of pregnancy status in rabbits. Estrogen regulates innate immune response both in a dose- and context-dependent manner (46). Reports have shown that IFN-λ protects the female reproductive tract against RNA viral infection and estrogen treatment protected against intravaginal infection (47), and long-term exposures to estrogen have positive regulatory effects on type-I IFN in females (48). Increased type-I IFN response was observed upon TLR7 ligand activation in women compared to men (49). In the mice model, administration of a higher dose of estrogen protected female mice against excessive inflammatory damage in the lungs (50). Ex vivo stimulation of peripheral blood mononuclear cells (PBMCs) with poly(I·C) (TLR3 ligand), LPS (TLR4 ligand), and R848 (TLR7/8 ligand) from HEV-infected pregnant women induced higher levels of IFN-α compared to PBMCs from HEV-infected nonpregnant women (43). Therefore, it should be taken into account that additional pathways may influence the HEV-induced innate immune response *in vivo* and that the *in vitro* Huh7-S10-3 liver cell model has its limitations in fully replicating the hormone flux environment seen in females. Another limitation of our *in vitro* study is the use of the HEV P6 strain, which has an insertion of host ribosomal protein S17 sequence in its genome and thus enables cell culture adaptation (28), while wild-type HEV strains lack this insertion. Unfortunately, other HEV strains, especially genotype 1 HEV, cannot be efficiently propagated in cell culture to allow us to perform the experiments.

In conclusion, our *in vitro* model based on 17β-estradiol treatment of Huh7-S10-3 human liver cells overexpressing the functional estrogen receptor ERαp66 did not lead to a significant increase in HEV replication. However, we demonstrate that STAT3 inhibition significantly reduced HEV ORF2 protein level and the immunomodulatory SOCS3 protein. We found that the estrogen classical signaling pathway via ERαp66 led to stabilization of SOCS3, a negative regulator of interferon and proinflammatory host response, even during the presence of STAT3 activation inhibitor. Therefore, it is possible that the estrogen classical signaling pathway via ERαp66 might contribute to dampening the host innate immune response during HEV infection *in vitro*, although other factors might also influence the overall innate immune response during HEV infection in pregnant women.

MATERIALS AND METHODS

Cells, HEV infectious clone, antibodies, plasmids, and estrogen. The Huh7-S10-3 human liver cells (51), kindly provided by Suzanne U. Emerson (NIH, Bethesda, MD), were maintained in Dulbecco's minimal essential medium (DMEM; Gibco-Thermo Fisher, MA, USA), with 5% fetal bovine serum (FBS; Atlanta Biologicals-RnD Systems, MN, USA), 1$\times$ antibacterial-antimycotic (Gibco-Thermo Fisher, MA, USA), and 1$\times$ Minimal essential amino acids (Gibco-Thermo Fisher, MA, USA). The genotype 3 human HEV (Kernow P6 strain) infectious cDNA clone used in this study was described previously (28). The HEV P6 infectious genomic RNA was transcribed using mMESSAGE mMACHINE T7 *in vitro* transcription kit (Invitrogen-Thermo Fisher, MA, USA). The rabbit anti-human ERα, rabbit anti-human pSTAT3, and mouse anti-human STAT3 antibodies were purchased from Cell Signaling Technology (Danvers, MA, USA), and the mouse anti-human SOCS3 and rabbit anti-GFP antibodies were procured from Santa Cruz Biotechnology (Dallas, TX, USA). The mouse anti-human GAPDH antibody was procured from Invitrogen-Thermo Fisher

(Waltham, MA, USA). The plasmid pCMV-hERalpha (cat. no. 101141) was procured from Addgene (52). Cell culture grade estrogen 17β-estradiol was procured from Sigma (St. Louis, MO, USA), a stock of a 3.7-mM concentration was made in 100% ethanol, and aliquots were stored in −80°C until use. The In-solution STAT3 inhibitor (S3I-201) was procured from Sigma (cat. no. 573130-5MG; St. Louis, MO, USA), and aliquots were stored at −80°C until use.

Convenient liver tissues from HEV-infected and control pregnant and nonpregnant rabbits. A group of age-matched nonpregnant rabbits and pregnant rabbits at 7 days gestation were infected with a genotype 3 strain of rabbit HEV (isolate GDC9; NCBI accession no. FJ906895) from an unrelated study. At 4 weeks postinfection (wpi), samples of liver tissues from HEV-infected and control nonpregnant and pregnant rabbits were collected during necropsy and stored at −80°C. The convenient samples of liver tissues collected from HEV-infected nonpregnant (n = 7 uninfected and n = 7 HEV-infected) and pregnant (n = 8 uninfected and n = 8 HEV-infected) rabbits at 4 wpi were used in the present study to determine the differential SOCS3 and ISG15 responses in the liver of HEV-infected animals.

Transient overexpression of ERαp66 in Huh7-S10-3 cells. The Huh7-S10-3 cells were cultured in phenol-red free DMEM with 25 mM HEPES, 5% charcoal-stripped FBS, 1× antibacterial-anitmycotic, and 1× minimal-essential media (Gibco-Thermo Fisher, MA, USA) for 48 h. The cells were then trypsinized, seeded on a 6-well plate, and incubated at 37°C, 5% CO_2, for 18 h to obtain 60 to 70% confluence. The next day, the cells were transfected with 1 μg of pCMV-hERalpha or pcDNA-GFP (vector control) plasmid per well. After 24 h posttransfection, the pcDNA-GFP/pCMV-hERalpha-transfected cells were trypsinized using a mild cell-dissociating agent (0.05% trypsin, 0.005 M EDTA, prepared in cell culture grade DPBS, to avoid phenol-red contamination) and seeded on to 24-well plate (~70,000 cells/well, in final culture volume of 700 μl). The cells were treated with a specific concentration of estrogen as described below.

Estrogen treatment of Huh7-S10-3 cells. 17β-estradiol is the major estrogen in females. Physiological concentration of 17β-estradiol in human serum during uncomplicated pregnancy varies between 2 and 31 ng/ml (26). To test the effect of pregnancy-related 17β-estradiol levels on HEV replication, in this study we considered the following 17β-estradiol concentrations as a representation of different trimesters of pregnancy: 2 ng/ml (7.3 nM) for first trimester, 10 ng/ml (37 nM) for second trimester, and 20 ng/ml (73 nM) for third trimester. To avoid cross interference of other steroid hormones, care was taken to use phenol red-free media and charcoal-stripped FBS to culture the Huh7-S10-3 cells. Accordingly, the plain Huh7-S10-3 cells or pCMV-hERαp66- or pcDNA-GFP-transfected Huh7-S10-3 cells were plated in a 24-well plate at a concentration of 70,000 cells per well in a 700-μl volume of phenol-red free DMEM with supplements as mentioned above. Cell culture grade 17β-estradiol stock was serially diluted to a working stock of 730 nM, 370 nM, and 73 nM in endotoxin-free, phenol-red free DMEM with supplements, and 70 μl of diluted 17β-estradiol working stock was added to each well in a plate to achieve a final estrogen concentration of 73 nM, 37 nM, and 7.3 nM, respectively, in the cell culture media.

To determine if estrogen signaling is intact and pCMV-hER αp66 expression is functional, samples were collected at various time points postestrogen treatment to determine the estrogen-mediated nonclassical and classical pathways in Huh7-S10-3 cells.

Transfection of HEV RNA and estrogen treatment. Plain Huh7-S10-3 cells or pCMV-hERαp66- or pcDNA-GFP-transfected Huh7-S10-3 cells plated on a 24-well plate were treated with or without estrogen for 24 h as mentioned above. The next day, i.e., 24 h postestrogen treatment, the cells were transfected with HEV RNA (300 to 400 ng/well) using Lipofectamine 2000. Estrogen (concentration is indicated in figure legends) was then added to the medium. The samples were collected at various time points post-HEV RNA transfection to measure host response (both at protein, and RNA levels) and HEV ORF2 RNA and protein levels.

Western blot analysis. Huh7-S10-3 cells treated at various conditions in the presence or absence of 17β-estradiol and/or STAT3 inhibitor were collected at different time points using 1× RIPA buffer containing protease-phosphatase inhibitors. The cell lysate was clarified by centrifugation at 14,000 × g for 5 min at 4°C. Approximately 30 μg of clarified lysate was loaded per well and resolved using 4 to 20% SDS-PAGE gel. The separated proteins were then transferred onto a 0.45-μm PVDF membrane and blocked using 5% BSA in PBST (0.1% Tween20 in PBS). The membrane was then probed using anti-ERα (1:1,000 dilution), anti-GFP (1:2,000 dilution), anti-STAT3 (1:2,000 dilution), anti-pSTAT3 (1:1,000 dilution), anti-SOCS3 (1:1,000 dilution), anti-HEV ORF2 (1:1,000 dilution), and anti-GAPDH (1:5,000 dilution) antibodies. Bovine anti-rabbit-IgG-HRP (1:7,000 dilution) and goat anti-mouse-IgG-HRP (1:4,000 dilution) were used as secondary antibodies. The membrane was then developed using Luminol reagent (SCBT, CA, USA) and imaged using a Bio-Rad imaging system (Bio-Rad, CA, USA).

RT-qPCR for quantification of SOCS3, cytokine, and ISG15 mRNA expressions. Total cellular RNAs were extracted from Huh7-S10-3 cells using Tri-Reagent (MRC, OH, USA) as per the manufacturer's protocol. The extracted RNAs were then treated with Turbo-DNase (Invitrogen-Thermo Fisher, MA, USA) and precipitated using Lithium Chloride (Invitrogen-Thermo Fisher, MA, USA) to obtain the purified RNA. The cDNA was synthesized from the purified RNA (500 ng/20-μl reaction volume) using a random hexamer and an ABI high-capacity cDNA kit from ABI-Thermo Fisher (Waltham, MA, USA). The mRNA levels of SOCS3, IFN-λ1, IL-6, and ISG15 were quantified from the cDNAs using ABI Power Sybr green qPCR mix (ABI-Thermo Fisher, MA, USA) and cytokine gene-specific primers (Table 2). The qPCR condition was 95°C for 2 min, followed by 40 cycles of 95°C for 5 s, 60°C for 10 s, and 72°C for 20 s.

RT-qPCR for quantification of negative-strand HEV RNA. To detect the amount of intracellular negative-strand HEV RNA that is indicative of HEV replication, cDNA was synthesized from the purified total cellular RNAs using ABI high-capacity cDNA kit with Tag + HEV-FP primer (Table 2). The HEV negative-strand qPCR was then carried out using the cDNA with a Sensifast No-ROX probe kit (Bioline-Thomas Scientific, NJ, USA) with primer pairs Tag and HEV-RP, and a HEV probe (Table 2). The qPCR

TABLE 2 Oligonucleotide primers used in this study[a]

Primer ID	Sequence (5′–3′)	Purpose
IFN-λ1 FP	AAAAAGGAGTCCGCTGGCTG	qPCR
IFN-λ1 RP	TCAGACACAGGTTCCCATCG	qPCR
ISG15 FP	GTGGACAAATGCGACGAACC	qPCR
ISG15 RP	TCGAAGGTCAGCCAGAACAG	qPCR
SOCS3 FP	GATTCGGGACCAGCCCCC	qPCR
SOCS3 RP	GCTGGTACTCGCTCTTGGAG	qPCR
IL-6 FP	CAATGAGGAGACTTGCCTGG	qPCR
IL-6 RP	TGGGTCAGGGGTGGTTATTG	qPCR
RPS18 FP	TGATCCCTGAAAAGTTCCAGCA	qPCR
RPS18 RP	CTTCGGCCCACACCCTTAAT	qPCR
Rabbit SOCS3 FP	CGTGGATTCGCCTCCTTTCT	qPCR
Rabbit SOCS3 RP	CAACCTGCTCGGCCTTAAAC	qPCR
Rabbit ISG15 FP	GTGACAACCCGCTGAGCATC	qPCR
Rabbit ISG15 RP	CTCGAAGCTCAGCCAGAACAG	qPCR
Rabbit RPS18 FP	ACTGCCATTAAGGGTGTGGG	qPCR
Rabbit RPS18 RP	CTTGTACTGACGCGGGTTCT	qPCR
Tag + HEV-FP	CGGTCATGGTGGCGAATAAGGTG[b] GTTTCTGGGGTGAC	HEV-ve strand cDNA synthesis
Tag	CGGTCATGGTGGCGAATAA	HEV-ve strand qPCR FP
HEV-FP	GGTGGTTTCTGGGGTGAC	HEV qPCR
HEV-RP	AGGGGTTGGTTGGATGAA	HEV qPCR
HEV-probe	5′FAM/TGATTCTCAGCCCTTCGC/3′BHQ	HEV qPCR

[a]FP, forward primter; RP, reverse primer.
[b]The underlined is the tag sequence in primer tag+HEV-FP.

condition included 95°C for 2 min, followed by 40 cycles of 95°C for 5 s, and 60°C for 30 s. No RT control and no template controls were included during each qPCR run.

Statistical analysis. Statistical comparison was performed using JMP Pro 16 (Cary, NC, USA). Analysis of variance (ANOVA) with a *post hoc* Student's *t* test or Tukey test was used. An *F* test was used to compare the convenient rabbit liver samples. $P \leq 0.05$ was considered significant.

SUPPLEMENTAL MATERIAL

Supplemental material is available online only.

SUPPLEMENTAL FILE 1, PDF file, 0.5 MB.

ACKNOWLEDGMENTS

The work is funded by a grant from the National Institutes of Health (R01 AI050611).

We thank Stephen Were for statistical analysis. The Huh7-S10-3 human liver cells and the genotype 3 human HEV (Kernow P6 strain) infectious cDNA clone used in this study were kindly provided by Suzanne U. Emerson (NIH, Bethesda, MD).

REFERENCES

1. Purdy MA, Harrison TJ, Jameel S, Meng XJ, Okamoto H, Van der Poel WHM, Smith DB, Ictv Report Consortium. 2017. ICTV virus taxonomy profile: Hepeviridae. J Gen Virol 98:2645–2646. https://doi.org/10.1099/jgv.0.000940.
2. Purdy MA, Khudyakov YE. 2011. The molecular epidemiology of hepatitis E virus infection. Virus Res 161:31–39. https://doi.org/10.1016/j.virusres.2011.04.030.
3. Smith DB, Izopet J, Nicot F, Simmonds P, Jameel S, Meng XJ, Norder H, Okamoto H, van der Poel WHM, Reuter G, Purdy MA. 2020. Update: proposed reference sequences for subtypes of hepatitis E virus (species Orthohepevirus A). J Gen Virol 101:692–698. https://doi.org/10.1099/jgv.0.001435.
4. Lhomme S, Marion O, Abravanel F, Izopet J, Kamar N. 2020. Clinical manifestations, pathogenesis and treatment of hepatitis E virus infections. J Clin Med 9:331. https://doi.org/10.3390/jcm9020331.
5. Sooryanarain H, Meng XJ. 2019. Hepatitis E virus: reasons for emergence in humans. Curr Opin Virol 34:10–17. https://doi.org/10.1016/j.coviro.2018.11.006.
6. Perez-Gracia MT, Suay-Garcia B, Mateos-Lindemann ML. 2017. Hepatitis E and pregnancy: current state. Rev Med Virol 27:e1929. https://doi.org/10.1002/rmv.1929.
7. Horvatits T, Schulze Zur Wiesch J, Lutgehetmann M, Lohse AW, Pischke S. 2019. The clinical perspective on hepatitis E. Viruses 11:617. https://doi.org/10.3390/v11070617.
8. Li M, Li S, He Q, Liang Z, Wang L, Wang Q, Wang L. 2019. Hepatitis E-related adverse pregnancy outcomes and their prevention by hepatitis E vaccine in a rabbit model. Emerg Microbes Infect 8:1066–1075. https://doi.org/10.1080/22221751.2019.1643260.
9. Xia J, Liu L, Wang L, Zhang Y, Zeng H, Liu P, Zou Q, Wang L, Zhuang H. 2015. Experimental infection of pregnant rabbits with hepatitis E virus demonstrating high mortality and vertical transmission. J Viral Hepat 22:850–857. https://doi.org/10.1111/jvh.12406.
10. Yang C, Yu W, Bi Y, Long F, Li Y, Wei D, Hao X, Situ J, Zhao Y, Huang F. 2018. Increased oestradiol in hepatitis E virus-infected pregnant women promotes viral replication. J Viral Hepat 25:742–751. https://doi.org/10.1111/jvh.12865.

11. Fuentes N, Silveyra P. 2019. Estrogen receptor signaling mechanisms. Adv Protein Chem Struct Biol 116:135–170. https://doi.org/10.1016/bs.apcsb.2019.01.001.
12. Gong S, Hao X, Bi Y, Yang C, Wang W, Mickael HK, Zhang Y, Chen S, Qian Z, Huang F, Wei D, Yu W. 2021. Hepatitis E viral infection regulates estrogen signaling pathways: inhibition of the cAMPK-PKA-CREB and PI3K-AKT-mTOR signaling pathways. J Med Virol 93:3769–3778. https://doi.org/10.1002/jmv.26641.
13. O'Lone R, Frith MC, Karlsson EK, Hansen U. 2004. Genomic targets of nuclear estrogen receptors. Mol Endocrinol 18:1859–1875. https://doi.org/10.1210/me.2003-0044.
14. Vrtacnik P, Ostanek B, Mencej-Bedrac S, Marc J. 2014. The many faces of estrogen signaling. Biochem Med (Zagreb) 24:329–342. https://doi.org/10.11613/BM.2014.035.
15. Qiu S, Vazquez JT, Boulger E, Liu H, Xue P, Hussain MA, Wolfe A. 2017. Hepatic estrogen receptor alpha is critical for regulation of gluconeogenesis and lipid metabolism in males. Sci Rep 7:1661. https://doi.org/10.1038/s41598-017-01937-4.
16. Shen M, Shi H. 2016. Estradiol and Estrogen receptor agonists oppose oncogenic actions of leptin in HepG2 cells. PLoS One 11:e0151455. https://doi.org/10.1371/journal.pone.0151455.
17. Tolomeo M, Cascio A. 2021. The multifaced role of STAT3 in cancer and its implication for anticancer therapy. Int J Mol Sci 22:603. https://doi.org/10.3390/ijms22020603.
18. Tsai MH, Pai LM, Lee CK. 2019. Fine-tuning of type I interferon response by STAT3. Front Immunol 10:1448. https://doi.org/10.3389/fimmu.2019.01448.
19. Ho HH, Ivashkiv LB. 2006. Role of STAT3 in type I interferon responses. Negative regulation of STAT1-dependent inflammatory gene activation. J Biol Chem 281:14111–14118. https://doi.org/10.1074/jbc.M511797200.
20. Chandra V, Kar-Roy A, Kumari S, Mayor S, Jameel S. 2008. The hepatitis E virus ORF3 protein modulates epidermal growth factor receptor trafficking, STAT3 translocation, and the acute-phase response. J Virol 82:7100–7110. https://doi.org/10.1128/JVI.00403-08.
21. Williams L, Bradley L, Smith A, Foxwell B. 2004. Signal transducer and activator of transcription 3 is the dominant mediator of the anti-inflammatory effects of IL-10 in human macrophages. J Immunol 172:567–576. https://doi.org/10.4049/jimmunol.172.1.567.
22. Leong GM, Moverare S, Brce J, Doyle N, Sjögren K, Dahlman-Wright K, Gustafsson J-A, Ho KKY, Ohlsson C, Leung K-C. 2004. Estrogen up-regulates hepatic expression of suppressors of cytokine signaling-2 and -3 in vivo and in vitro. Endocrinology 145:5525–5531. https://doi.org/10.1210/en.2004-0061.
23. Leslie K, Lang C, Devgan G, Azare J, Berishaj M, Gerald W, Kim YB, Paz K, Darnell JE, Albanese C, Sakamaki T, Pestell R, Bromberg J. 2006. Cyclin D1 is transcriptionally regulated by and required for transformation by activated signal transducer and activator of transcription 3. Cancer Res 66:2544–2552. https://doi.org/10.1158/0008-5472.CAN-05-2203.
24. Foster JS, Wimalasena J. 1996. Estrogen regulates activity of cyclin-dependent kinases and retinoblastoma protein phosphorylation in breast cancer cells. Mol Endocrinol 10:488–498. https://doi.org/10.1210/mend.10.5.8732680. https://doi.org/10.1210/me.10.5.488.
25. Mahsoub HM, Heffron CL, Sooryanarain H, Hassebroek AM, Wang B, LeRoith T, Meng XJ. 2022. Hepatitis E virus causes fetal loss in pregnant rabbits which corresponds to upregulation of liver inflammatory cytokines, p 7. Proceeding of the American Society for Virology 41st Annual Meeting. Madison, WI.
26. Schock H, Zeleniuch-Jacquotte A, Lundin E, Grankvist K, Lakso HA, Idahl A, Lehtinen M, Surcel HM, Fortner RT. 2016. Hormone concentrations throughout uncomplicated pregnancies: a longitudinal study. BMC Pregnancy Childbirth 16:146. https://doi.org/10.1186/s12884-016-0937-5.
27. Jilani N, Das BC, Husain SA, Baweja UK, Chattopadhya D, Gupta RK, Sardana S, Kar P. 2007. Hepatitis E virus infection and fulminant hepatic failure during pregnancy. J Gastroenterol Hepatol 22:676–682. https://doi.org/10.1111/j.1440-1746.2007.04913.x.
28. Shukla P, Nguyen HT, Faulk K, Mather K, Torian U, Engle RE, Emerson SU. 2012. Adaptation of a genotype 3 hepatitis E virus to efficient growth in cell culture depends on an inserted human gene segment acquired by recombination. J Virol 86:5697–5707. https://doi.org/10.1128/JVI.00146-12.
29. Miceli V, Cocciadiferro L, Fregapane M, Zarcone M, Montalto G, Polito LM, Agostara B, Granata OM, Carruba G. 2011. Expression of wild-type and variant estrogen receptor alpha in liver carcinogenesis and tumor progression. OMICS 15:313–317. https://doi.org/10.1089/omi.2010.0108.
30. Zhang J, Ren J, Wei J, Chong CC, Yang D, He Y, Chen GG, Lai PB. 2016. Alternative splicing of estrogen receptor alpha in hepatocellular carcinoma. BMC Cancer 16:926. https://doi.org/10.1186/s12885-016-2928-3.
31. Wang Z, Zhang X, Shen P, Loggie BW, Chang Y, Deuel TF. 2006. A variant of estrogen receptor-{alpha}, hER-{alpha}36: transduction of estrogen- and antiestrogen-dependent membrane-initiated mitogenic signaling. Proc Natl Acad Sci U S A 103:9063–9068. https://doi.org/10.1073/pnas.0603339103.
32. Duong V, Licznar A, Margueron R, Boulle N, Busson M, Lacroix M, Katzenellenbogen BS, Cavailles V, Lazennec G. 2006. ERalpha and ERbeta expression and transcriptional activity are differentially regulated by HDAC inhibitors. Oncogene 25:1799–1806. https://doi.org/10.1038/sj.onc.1209102.
33. Gouilly J, Chen Q, Siewiera J, Cartron G, Levy C, Dubois M, Al-Daccak R, Izopet J, Jabrane-Ferrat N, El Costa H. 2018. Genotype specific pathogenicity of hepatitis E virus at the human maternal-fetal interface. Nat Commun 9:4748. https://doi.org/10.1038/s41467-018-07200-2.
34. Roca Suarez AA, Van Renne N, Baumert TF, Lupberger J. 2018. Viral manipulation of STAT3: evade, exploit, and injure. PLoS Pathog 14:e1006839. https://doi.org/10.1371/journal.ppat.1006839.
35. Hosel M, Quasdorff M, Ringelhan M, Kashkar H, Debey-Pascher S, Sprinzl MF, Bockmann JH, Arzberger S, Webb D, von Olshausen G, Weber A, Schultze JL, Buning H, Heikenwalder M, Protzer U. 2017. Hepatitis B virus activates signal transducer and activator of transcription 3 supporting hepatocyte survival and virus replication. Cell Mol Gastroenterol Hepatol 4:339–363. https://doi.org/10.1016/j.jcmgh.2017.07.003.
36. Sen N, Che X, Rajamani J, Zerboni L, Sung P, Ptacek J, Arvin AM. 2012. Signal transducer and activator of transcription 3 (STAT3) and survivin induction by varicella-zoster virus promote replication and skin pathogenesis. Proc Natl Acad Sci U S A 109:600–605. https://doi.org/10.1073/pnas.1114232109.
37. Villa A, Rizzi N, Vegeto E, Ciana P, Maggi A. 2015. Estrogen accelerates the resolution of inflammation in macrophagic cells. Sci Rep 5:15224. https://doi.org/10.1038/srep15224.
38. Wang H, Yuan M, Wang S, Zhang L, Zhang R, Zou X, Wang X, Chen D, Wu Z. 2019. STAT3 regulates the type I IFN-mediated antiviral response by interfering with the nuclear entry of STAT1. Int J Mol Sci 20:4870. https://doi.org/10.3390/ijms20194870.
39. Yin X, Li X, Ambardekar C, Hu Z, Lhomme S, Feng Z. 2017. Hepatitis E virus persists in the presence of a type III interferon response. PLoS Pathog 13:e1006417. https://doi.org/10.1371/journal.ppat.1006417.
40. Sooryanarain H, Heffron CL, Meng XJ. 2020. The U-Rich Untranslated Region of the Hepatitis E virus induces differential type I and type III interferon responses in a host cell-dependent manner. mBio 11:e03103-19. https://doi.org/10.1128/mBio.03103-19.
41. Wang W, Wang Y, Qu C, Wang S, Zhou J, Cao W, Xu L, Ma B, Hakim MS, Yin Y, Li T, Peppelenbosch MP, Zhao J, Pan Q. 2018. The RNA genome of hepatitis E virus robustly triggers an antiviral interferon response. Hepatology 67:2096–2112. https://doi.org/10.1002/hep.29702.
42. Murata K, Kang JH, Nagashima S, Matsui T, Karino Y, Yamamoto Y, Atarashi T, Oohara M, Uebayashi M, Sakata H, Matsubayashi K, Takahashi K, Arai M, Mishiro S, Sugiyama M, Mizokami M, Okamoto H. 2020. IFN-lambda3 as a host immune response in acute hepatitis E virus infection. Cytokine 125:154816. https://doi.org/10.1016/j.cyto.2019.154816.
43. Arya RP, Arankalle VA. 2014. Toll like receptors in self-recovering hepatitis E patients with or without pregnancy. Hum Immunol 75:1147–1154. https://doi.org/10.1016/j.humimm.2014.10.011.
44. Sehgal R, Patra S, David P, Vyas A, Khanam A, Hissar S, Gupta E, Kumar G, Kottilil S, Maiwall R, Sarin SK, Trehanpati N. 2015. Impaired monocyte-macrophage functions and defective Toll-like receptor signaling in hepatitis E virus-infected pregnant women with acute liver failure. Hepatology 62:1683–1696. https://doi.org/10.1002/hep.28143.
45. Knegendorf L, Drave SA, Dao Thi VL, Debing Y, Brown RJP, Vondran FWR, Resner K, Friesland M, Khera T, Engelmann M, Bremer B, Wedemeyer H, Behrendt P, Neyts J, Pietschmann T, Todt D, Steinmann E. 2018. Hepatitis E virus replication and interferon responses in human placental cells. Hepatol Commun 2:173–187. https://doi.org/10.1002/hep4.1138.
46. Kovats S. 2015. Estrogen receptors regulate innate immune cells and signaling pathways. Cell Immunol 294:63–69. https://doi.org/10.1016/j.cellimm.2015.01.018.
47. Caine EA, Scheaffer SM, Arora N, Zaitsev K, Artyomov MN, Coyne CB, Moley KH, Diamond MS. 2019. Interferon lambda protects the female reproductive tract against Zika virus infection. Nat Commun 10:280. https://doi.org/10.1038/s41467-018-07993-2.
48. Laffont S, Rouquie N, Azar P, Seillet C, Plumas J, Aspord C, Guery JC. 2014. X-Chromosome complement and estrogen receptor signaling

independently contribute to the enhanced TLR7-mediated IFN-alpha production of plasmacytoid dendritic cells from women. J Immunol 193:5444–5452. https://doi.org/10.4049/jimmunol.1303400.
49. Berghofer B, Frommer T, Haley G, Fink L, Bein G, Hackstein H. 2006. TLR7 ligands induce higher IFN-alpha production in females. J Immunol 177:2088–2096. https://doi.org/10.4049/jimmunol.177.4.2088.
50. Robinson DP, Hall OJ, Nilles TL, Bream JH, Klein SL. 2014. 17beta-estradiol protects females against influenza by recruiting neutrophils and increasing virus-specific CD8 T cell responses in the lungs. J Virol 88:4711–4720. https://doi.org/10.1128/JVI.02081-13.
51. Emerson SU, Nguyen HT, Torian U, Burke D, Engle R, Purcell RH. 2010. Release of genotype 1 hepatitis E virus from cultured hepatoma and polarized intestinal cells depends on open reading frame 3 protein and requires an intact PXXP motif. J Virol 84:9059–9069. https://doi.org/10.1128/JVI.00593-10.
52. Mao C, Patterson NM, Cherian MT, Aninye IO, Zhang C, Montoya JB, Cheng J, Putt KS, Hergenrother PJ, Wilson EM, Nardulli AM, Nordeen SK, Shapiro DJ. 2008. A new small molecule inhibitor of estrogen receptor alpha binding to estrogen response elements blocks estrogen-dependent growth of cancer cells. J Biol Chem 283:12819–12830. https://doi.org/10.1074/jbc.M709936200.